ACS APPLIED MATERIALS & INTERFACES
Research Article
www.acsami.org

Elastomeric Angled Microflaps with Reversible Adhesion for Transfer-Printing Semiconductor Membranes onto Dry Surfaces

Byungsuk Yoo,[†] Sungbum Cho,[†] Seungwan Seo,[†] and Jongho Lee*,[†,‡]

[†]Gwangju Institute of Science and Technology (GIST), Mechatronics, 123 Cheomdan-gwagiro, Buk-gu, Gwangju 500-712, South Korea

[‡]Gwangju Institute of Science and Technology (GIST), Research Institute of Solar and Sustainable Energies (RISE), 123 Cheomdan-gwagiro, Buk-gu, Gwangju 500-712, South Korea

S *Supporting Information*

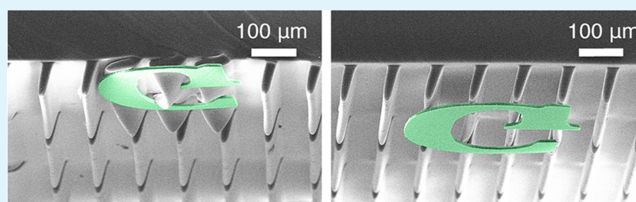

ABSTRACT: Recent research for unconventional types of electronics has revealed that it is necessary to transfer-print high-performance microelectronic devices onto diverse surfaces, including flexible or stretchable surfaces, to relieve mechanical constraints associated with conventional rigid electronics. Picking up and placing ultrathin microdevices without damage are critical procedures for the successful manufacture of various types of unconventional electronics. This paper introduces elastomeric angled microflaps that have reversible adhesion; i.e., they generate higher adhesion for picking up and low adhesion for printing because of their structural shapes and viscoelastic material properties. The microstructured stamp, fabricated in relatively simple ways, enables simultaneous transfer-printing of multiple silicon membranes that have irregular shapes in sizes ranging from micrometer to millimeter scales. Mechanical characterizations by experiment reveal optimal parameters for picking up and placing ultrathin membranes on a programmable custom-built microstage. Further refinement of the structures and materials should be useful for many applications requiring the microassembly of multiple semiconductor membranes in diverse shapes and sizes on dry surfaces without the aid of liquid adhesives.

KEYWORDS: *transfer-printing, microassembly, adhesion, biomimetics*

INTRODUCTION

Recent research on unconventional electronics has opened the possibility of expanding the use of high-performance electronics for much more diverse applications such as flexible displays,[1−3] stretchable photovoltaics,[4,5] biointegrated electronics,[6−8] and many others,[9,10] which are not achievable with the conventional type of electronics, often because of mechanical constraints, e.g., flat, rigid, or brittle elements. A promising method to realize unconventional electronics is to combine inorganic semiconductor devices, whose electronic performance has been improved over several decades,[11,12] with substrates that have mechanical properties that meet the requirements for specific applications in a way that isolates thin semiconductor devices from the original semiconductor substrates and prints the devices on target substrates. These hybrid-type electronics maintain high electrical performances with the required mechanical properties associated with target substrates.

One of the critical challenges in realizing the hybrid-type electronics is to pick ultrathin semiconductor devices from the original substrates and to integrate them with target substrates using a bulk elastomeric stamp, e.g., a smooth tacky poly(dimethylsiloxane) (PDMS) stamp (elastic modulus of about 1.8 MPa);[13] that process makes it challenging to release the ultrathin electronics devices without liquid adhesive layers on the target substrates. Liquid adhesive layers may cause physical flow or drying out during the transfer-printing procedure and require thermal processing or ultraviolet (UV) illumination for curing after or during transfer-printing.[14] In addition, the adhesive layers generally increase the thermal or electrical resistance between the devices and substrates.[15,16]

One approach to address these limitations is to use controllable adhesives, which were inspired by biological systems such as geckos.[17,18] Gecko-inspired adhesives provide reversible smart adhesion for diverse applications, such as medical tapes, climbing robots, and many others.[19−34] Some adhesives provide reversible adhesive characteristics depending on the unique structures or manipulations for transfer-printing.[35−40] These structured adhesives generate adhesion high enough to pick up thin membranes and reduced adhesion to retrieve them on dry surfaces. However, no structured adhesive has demonstrated transfer-printing of multiple semiconductor membranes at various scales at one time without extra actuators. A versatile adhesive stamp is a critically important tool for manufacturing large-scale unconventional electronics efficiently. Here, we present an adhesive stamp, prepared with elastomeric materials in scalable ways, that enables automated transfer-printing of multiple ultrathin semiconductor membranes with irregular shapes in sizes

Received: August 7, 2014
Accepted: October 9, 2014
Published: October 21, 2014

 © 2014 American Chemical Society dx.doi.org/10.1021/am505286b | *ACS Appl. Mater. Interfaces* 2014, 6, 19247−19253

ranging from micrometer to millimeter scale. We describe the preparation methods for the adhesive stamp, called an angled microflap array, along with mechanical characterization by experiment. Finally, we show how the silicon (Si) membranes can be rearranged with different spacing and describe the transfer-printing of various shaped and sized ultrathin semiconductor membranes in an automated way on a custom-built motorized microstage. This approach improves the efficiency of transfer-printing of multiple Si membranes in diverse shapes and sizes without replacing the adhesive stamp.

■ RESULTS AND DISCUSSION

Figure 1 shows a schematic illustration of the fabrication procedure and images of the master mold and angled microflap array. The procedure begins with spin-casting and curing of a relatively thin layer of negative photoresist (PR; thickness ~30 μm, SU8, Microchem) on a transparent glass substrate, followed by further spin-casting of a relatively thick negative PR layer (thickness ~80 μm, SU8). The thin SU8 layer serves as an adhesive layer on the glass substrate. The transparent glass substrate reduces reflection, which causes undesirable exposure of the PR along with photolithographic patterning of the SU8 layer in an angled configuration. Figure 1a shows UV exposure of the masked SU8 layer in an angled configuration at 60° from the surface of the PR, followed by another exposure at 45°, as illustrated in Figure 1b. This method of exposure of the PR layer twice from only one side is relatively simple because it does not require replacement or alignment of the mask. Post-exposure baking (PEB) and development of the unexposed regions, which generates cavities in the shape of slanted triangles, completes the fabrication process of the master mold; the scanning electron microscopy (SEM) image in Figure 1c clearly shows the slanted triangles. Although the master mold can be scaled up depending on the UV exposure systems, we confined the size of the master mold to 2 cm × 2 cm. The casting and curing methods of soft lithography[13,41] with a mixture of silicone elastomer base and curing agent (10:1, Sylgard 184, Dow Corning) in the master mold form elastomer replicas (PDMS) of the angled microflap array. The SEM image in Figure 1d provides a cross-sectional view of the angled microflaps with surfaces angled about 72° and 65° from the backing layer. Snell's law[42] estimates the angles (72° and 65°) of UV in the PR (refractive index n = 1.668 at λ = 365 nm)[43] from the angles of the incident UV light (60° and 45°) in the air (refractive index n = 1.0003 at λ = 365 nm and T = 20 °C).[44] The angles determine the height (h = 70 μm) of the microflaps from the thickness at the root (t = 25 μm) of each microflap (aspect ratio 2.8). The width (w) and space (s) of the microflaps are 500 and 75 μm, respectively. The Experimental Section and Supporting Information (SI) provide more details of the fabrication process.

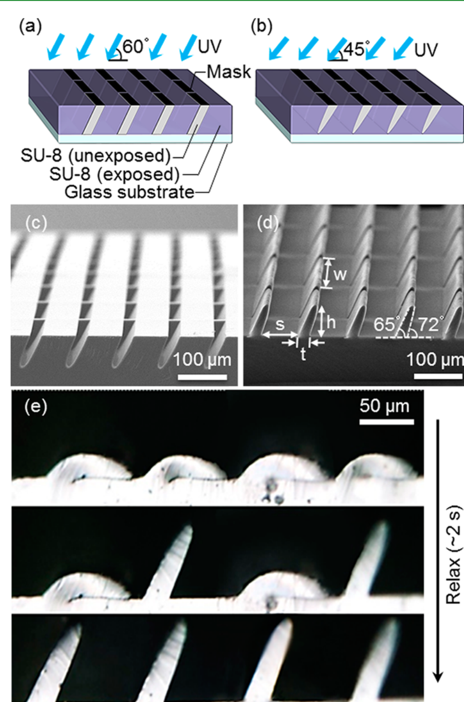

Figure 1. Schematic illustrations of the fabrication process and images of the master mold and angled microflap array. (a) First exposure of the masked SU8 layer at 60° spun on a transparent glass substrate. The transparent glass substrate reduces reflection on the surface, minimizing undesirable exposure by the reflected light. (b) Second exposure at 45° forming unexposed, slanted, triangular cross-sectional regions that will be removed in the developing process. The second exposure does not require an additional mask or realignment of the mask. (c) SEM image of the master mold after development of the unexposed regions followed by PEB. The image shows the angled recesses. (d) SEM image of the angled microflap array produced by casting and curing of a mixture of silicone elastomer base and curing agent (10:1, Sylgard 184, Dow Corning) into the master mold (2 cm × 2 cm). The angles of both surfaces of the microflaps are about 72° and 65° measured counterclockwise from the base. The thickness at the root and height and width of each microflap are 25, 70, and 500 μm, respectively. (e) Sequential images of the angled microflap array recovery from the collapsed to original configuration. It takes about less than 2 s to fully recover the original configuration.

The angled microflaps are tacky and elastic (E = 1.8 MPa) with an aspect ratio of height/thickness = 70/25 = 2.8. They collapse to the base when a vertical load is applied, but they recover their original shapes when the load is removed because of the viscoelastic properties of the elastomeric structure, as shown in Figure 1e. The optical microscopy images, taken sequentially for 2 s, show the angled microflap recovery from the collapsed configuration. Initially, the collapsed microflaps provide relatively large plane surfaces (top image in Figure 1e), but the outermost area decreases drastically until finally there are just the tips of the microflaps, when the microflaps recover the original shape when relaxed (last image in Figure 1e).

Transfer-printing of thin microdevices such as solar cells, light-emitting diodes (LEDs), transistors, and others is one of key technologies in manufacturing high-performance electronics in flexible, stretchable forms for diverse applications, including wearable and biointegrated electronics. Transfer-printing requires high adhesion when picking up devices and low adhesion when placing, i.e., printing, the devices on target surfaces many times without leaving glue layers on the target surfaces. We use the angled microflap array for the transfer-printing of thin micrometer-scale semiconductor materials (Si), prepared with a Si-on-insulator (SOI) wafer by removing the buried oxide layer (SiO_2; thickness 1 μm) with wet chemical etching [hydrofluoric acid (HF); J. T. Baker] after laterally defining and temporarily holding the top Si (capital letter G; size 400 μm × 450 μm; thickness 7 μm) with a breakable PR (AZ5214) as described elsewhere.[40] The Experimental Section provides more details. From now on, we call the angled microflap array an "angled microflap stamp".

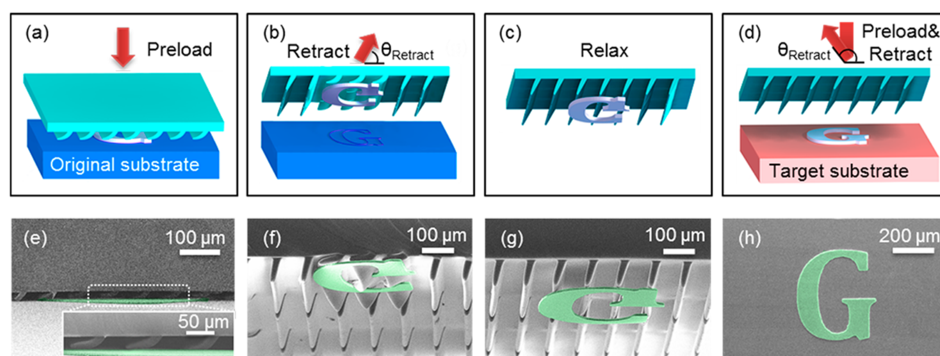

Figure 2. Schematic illustrations and SEM images of the transfer-printing procedure using the angled microflap stamp. (a) Schematic illustration of the angled microflap array approach to make contact with the micrometer-scale Si membrane that is prepared with SOI wafers. Dry etching defines the lateral layouts. Breakable anchors temporarily hold the micrometer-scale Si membrane after wet chemical etching removes the underlying SiO_2 layer. (b) Retraction of the array of the collapsed microflaps picking up the micrometer-scale Si membrane from the original substrate. The microflaps remain collapsed right after retraction. (c) Within about 2 s after retraction, the angled microflap array recovering its original shape, leaving only a small contact (tip contact) with the micrometer-scale Si membrane. (d) Schematic illustration of printing of the micrometer-scale Si membrane onto the receiver substrate. After the micrometer-scale Si membrane is brought into contact with the receiver substrate, retracting the angled microflap array slowly leaves the micrometer-scale Si membrane on the receiver substrate. (e) SEM image of the angled microflap array making contact with the micrometer-scale Si membrane (capital letter G; size 400 μm × 450 μm; thickness 7 μm). (f) SEM image, taken after UV ozone treatment for imaging, indicating that the angle microflaps make side contact with the micrometer-scale Si membranes. (g) Recovered microflaps after relaxation. (h) Micrometer-scale Si membrane printed on the dry receiver substrate without any adhesive layers between the micrometer-scale Si membrane and receiver substrate.

Parts a−d of Figure 2 show the schematic illustration of the transfer-printing procedure of the micrometer-scale Si membrane using the angled microflap stamp. We first preload the angled microflap stamp on a manual translation stage to make contact with the micrometer-scale Si membrane on the original substrate, as shown in Figure 2a. The angled microflaps collapse and make side contact with the micrometer-scale Si membrane, maximizing adhesion. Retracting the angled microflap stamp quickly retrieves the micrometer-scale Si membrane from the original substrate, as illustrated in Figure 2b. The angled microflaps recover their original configuration within 2 s because of the viscoelastic properties of the elastomer, making only the tip contact the micrometer-scale Si membrane, as illustrated in Figure 2c. Finally, following preloading and retraction of the "inked" angled microflap stamp, the micrometer-scale Si membrane is slowly placed on the dry target substrate without any aid from wet glue layers. Parts e−h of Figure 2 show corresponding SEM images during the transfer-printing procedure for preloading (Figure 2e), retracting (Figure 2f), relaxing (Figure 2g), and finally printing (Figure 2h) on the target Si substrate.

A qualitative study by experiment characterizes the adhesive properties of the angled microflaps in different modes of manipulation: applied preloads, manipulation speeds, and retraction angles. Figure 3a shows the measurement results for normal and shear forces of the angled microflap stamp (5 mm × 5 mm) on a custom-built, motorized microstage (Cheungwon Electronics) equipped with a multiaxis force sensor (ATI Industrial Automation) and a stereoscopic microscope (Olympus). See more details in the Experimental Section and SI. During the measurement, the angled microflap stamp is preloaded in the normal direction (about −1 N, the negative sign means a compressive force), as plotted with a red solid line. Because the microflaps are angled, there is a compressive reaction force, plotted with a black dashed line, in the shear direction, although the angled microflap stamp is preloaded in the normal direction. Upon retraction of the angled microflap stamp at the desired angle (60° in this case) from the substrate, the normal and shear forces switch from a negative (compressive) to a positive (tensile, maximum normal force 0.23 N). The gravitational force (approximately 14.4 nN) of the Si membrane (G shape; size ∼0.09 mm^2; thickness 7 μm) is negligibly small (∼1/57500 times less) compared to the adhesive force (0.23 N × 0.09/25 = 830000 nN) of the angled microflap stamp (size ∼25 mm^2). The manipulation speed for both preloading and retraction is 200 μm/s. The adhesive force (tensile) depends on the applied preload. Figure 3b shows the normal adhesive force with respect to the applied preloads. With applied preloads of less than 2 N, the normal adhesive force increases as the preload increases. However, the normal adhesive force reaches a plateau (0.25 N) for preloads of higher than 2 N. The plateau is attributed to the contact area for the applied preloads, as shown in the SI (Figure S4). The optical images captured during preloading indicate that the contact area with the substrate increases as the applied preload increases but remains almost the same for higher preloads. The results indicate that a preload of around 1−2 N is enough for the maximum adhesive force. Since too much preload may damage ultrathin micrometer-scale membranes at picking up, for most cases, we applied a preload of 1 N, which is high enough to provide a similar level of adhesive force (0.23 N) comparable to the plateau (0.25 N).

The retraction speed is another important factor in determining the adhesive force, as indicated with the experimental results in Figure 3c. The experiment, conducted with a fixed preload (1 N) and retraction angle (60°) at various speeds (5−1000 μm/s), indicates that the normal adhesive force is proportional to the retraction speed because of the viscoelastic properties of the elastomeric material (PDMS; elastic modulus 1.8 MPa).[13] The results suggest retracting the angled microflap stamp at a relatively higher speed when picking up micrometer-scale Si membranes and at a relatively lower speed when placing them on substrates.

The asymmetric structure of the angled microflaps provides anisotropic adhesive properties depending on the retraction angles. Figure 3d shows the adhesive forces measured at

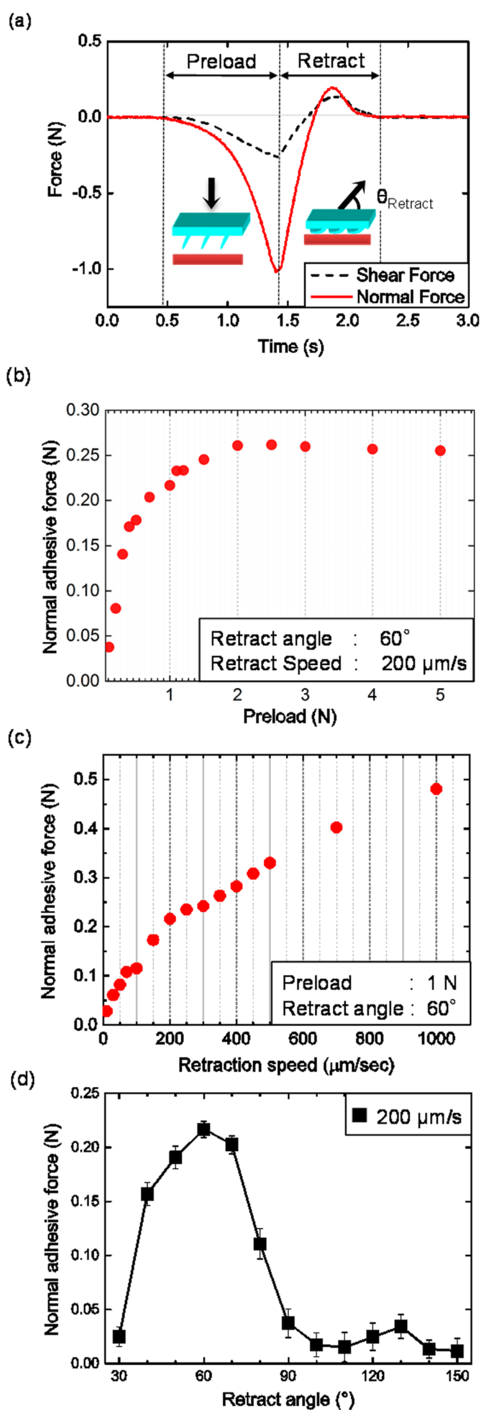

Figure 3. Measurement results of mechanical characteristics of the angled microflap stamp, depending on the preload, retraction speed, and retraction angle. (a) Measurement of the normal (red solid line) and shear (black dashed line) forces during preload and retraction of the angled microflap stamp (5 mm × 5 mm). The preload is applied vertically to the angled microflap array by −1 N. The negative sign indicates compression. The normal preload also causes a negative (compressive) shear load. During angled retraction ($\theta_{retract}$ = 60°), the compressive normal and shear forces change to tensile (adhesive) forces. The peak of the red line is the maximum normal adhesive force (0.23 N). The speed of the normal approach and angled retraction is 200 μm/s. (b) Normal adhesive force depending on the applied preloads when the angled microflap array is retracted ($\theta_{retract}$ = 60°) at a constant speed (200 μm/s). The normal adhesive force increases and reaches a plateau (0.25 N) for an applied preload higher than 2 N. (c) Normal adhesive force depending on the retraction speed for an

Figure 3. continued

applied preload of 1 N and retraction angle of 60°. The adhesive force is stronger at a higher speed because of the viscoelastic properties of the elastomeric material (elastic modulus 1.8 MPa). (d) Normal adhesive force depending on the retraction angle when preloaded by 1 N and retracted at 200 μm/s. The asymmetric geometry of the angled microflap array causes the anisotropic (directional) adhesive characteristics. The adhesive force is maximum at a retraction angle of 60° and decreases drastically at a retraction angle higher than 90°. The anisotropic adhesive characteristics suggest optimal retraction angles for picking up (around 60°) and placing (around 100°) the micrometer-scale Si membranes.

retraction at every 10° ranging from 30° to 150° for the fixed preload (1 N) and manipulation speed (200 μm/s). The adhesive force is relatively high (max 0.23 N) for retraction at an angle lower than 90° and relatively low at an angle higher than 90° (<0.025 N). The adhesive force (0.23 N) for retraction at 60° is almost 13 times that (0.017 N) for retraction at 100°. Those qualitative studies suggest using higher adhesion when picking up micrometer-scale Si membranes by retracting the angled microflap stamp at an angle of around 40−60° at a relatively high speed and using low adhesion when placing the membranes on a surface at an angle higher than 90° at relatively low speed.

With an angled microflap stamp, replicated from one master mold, transfer-printing thin Si membranes in various shapes and sizes is possible on a dry target surface using a custom-built microstage preprogrammed with parameters acquired from the mechanical characterization. On the basis of the quantitative studies of the angled microflap stamp, we programmed the custom-built motorized microstage to pick up thin Si membranes automatically by applying a preload of 1 N and retracting at 60° at a relatively high speed (200 μm/s) and to place the membranes by retracting at 100° at 50 μm/s, as illustrated in Figure 4a. Picking up and placing multiple membranes at the same time is efficient for the manufacture of large-scale arrays. Parts b and c of Figure 4 show the SEM images of multiple Si membranes (outer diameter 230 μm; inner diameter 90 and 125 μm; thickness 7 μm), picked up with the angled microflap stamp at the same time (Figure 4b) and placed on a dry Si substrate at the same time (Figure 4c). A microthickness Si slender bar (2 mm × 25 μm × 7 μm) is also transfer-printable with the angled microflap stamp without breaking the bar, as shown in Figure 4d,e.

As long as at least two angled microflaps support a Si membrane, as shown in Figure 4f, transfer-printing membranes in various sizes is also possible. Figure 4g shows the micrometer-scale Si membranes (capital letter G; largest one, 750 μm × 600 μm; smallest one, 100 μm × 80 μm) transfer-printed one by one on the dry Si substrate without switching the angled microflap stamp. The distance (75 μm) between microflaps limits the minimum size of the transfer-printable membranes because micrometer-scale Si membranes smaller than the space of the angled microflaps may become stuck between the microflaps. It will be necessary to redesign the microflap array to transfer-print smaller micrometer-scale Si membranes. Parts h and i of Figure 4 show the SEM images of the millimeter-scale Si membrane (a piece of capital letters "GIST"; 1.5 mm × 540 μm) transfer-printed on the dry target substrate. The last two SEM images in Figure 4 show multiple Si membranes in relatively complex, irregular shapes in sizes

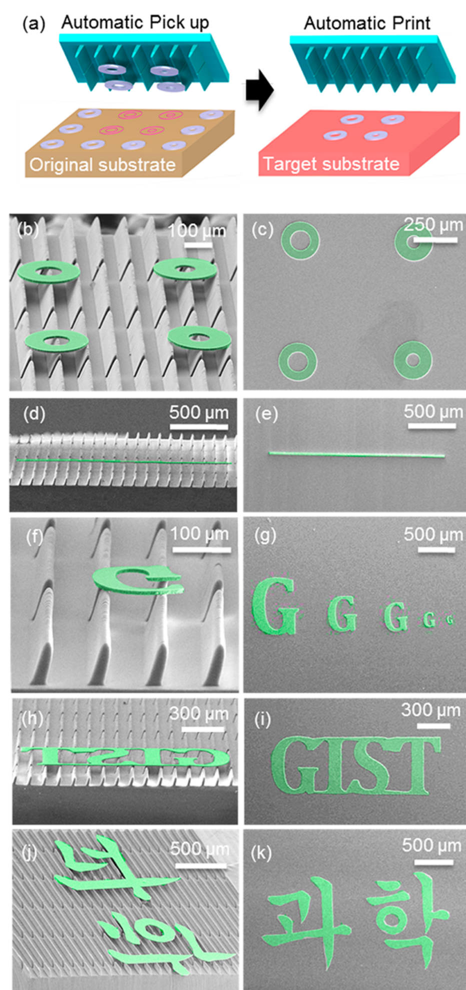

Figure 4. Images of various shapes and sizes of micrometer-scale Si membranes transfer-printed on dry target (Si) substrates with the angled microflap stamp on the motorized microstage. (a) Schematic illustration of the automated transfer-printing procedure from the original to target substrate. (b) Four micrometer-scale Si membranes (outer diameter 230 μm; inner diameter 90−125 μm; thickness 7 μm) picked up and (c) printed on the receiver substrate at the same time. (d and e) Slender Si bar (2 mm × 25 μm × 7 μm) transfer-printed using the angled microflap stamp. (f and g) Micrometer-scale Si membranes (letter G) in different sizes (largest one on the left, 750 μm × 600 μm; smallest one on the right, 100 μm × 80 μm) transfer-printed on the target substrate. The minimum size of the Si membrane is limited by the space (75 μm) between the angled microflaps. (h and i) Millimeter-scale Si membrane (a piece of capital letters "GIST"; size 1.5 mm × 540 μm) transfer-printed using the angled microflap stamp. (j and k) Multiple irregular-shaped Si membranes (Korea letters meaning "science", size 2.3 mm × 1.2 mm) picked and placed all together at one time.

from micrometer to millimeter scale (Korean letters meaning "science"; whole size, 2.3 mm × 1.2 mm; smallest, 290 μm × 125 μm; largest, 1.1 mm × 150 μm) picked up (Figure 4j) and placed on the target (Figure 4k) all together at one time on the motorized microstage.

Another functionality required for the manufacture of flexible or stretchable electronics is to pick micrometer-scale Si membranes and print them in different spaces, i.e., in higher or lower density. This functionality is useful for rearranging micrometer-scale Si membranes already printed, or making up for missing or damaged membranes, in addition to integrating micrometer-scale membranes fabricated in high density on the original substrate over a large area on the target substrate for efficient use of the materials. Representative results appear in Figure 5. Parts a and b of Figure 5 present a schematic illustration and optical microscope images of micrometer-scale Si membranes (outer diameter 580 μm; inner diameter 220−300 μm) transfer-printed on the target substrate in the same period (2 mm) as they were fabricated on the original substrate. The rearrangement of the micrometer-scale Si membranes by picking them up and printing them one by one in a higher period (4 mm) appears in Figure 5c,d. Parts e and f of Figure 5 show images of micrometer-scale Si membranes printed in a shorter period (1 mm) using the angled microflap stamp on the custom-built motorized microstage. The yield of transfer-printing is about 90% in the first trial on the current setup. The alignment accuracy of the micrometer-scale Si membranes is less than 4 μm, which can be improved further with a high-quality microscope and stage. See the SI for details.

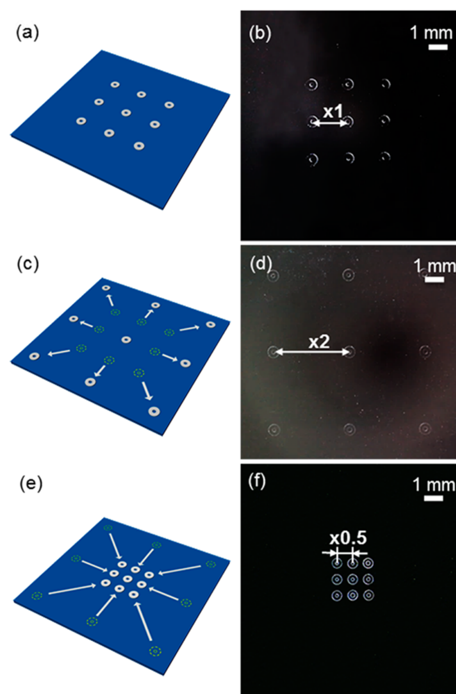

Figure 5. Schematic illustrations and optical images of the transfer-printing of micrometer-scale Si membranes (outer diameter 580 μm; inner diameter 220−300 μm) in various periods using the angled microflap stamp on the custom-built motorized microstage: (a and b) micrometer-scale Si membranes transfer-printed on the receiver substrate in the same period (2 mm) as the original substrate; (c and d) micrometer-scale Si membranes picked and placed in larger (4 mm) and (e and f) smaller periods (1 mm).

■ CONCLUSION

In conclusion, the adhesive stamp presented here for the transfer-printing of various shapes of multiple semiconductor membranes in sizes ranging from micrometer to millimeter scale on a dry surface provides advantages for the manufacture of large-scale unconventional electronics that require integration of high-performance semiconductor membranes, including solar cells, LEDs, sensors, and many others. The adhesive properties of the stamps, controllable by applied preloads, manipulation speeds, and retraction angles, are further

adjustable with additional refinements of the structures or replacement of the materials that have different mechanical or chemical properties. The relatively simple fabrication methods reported here should be useful for many applications.

■ EXPERIMENTAL SECTION

Fabricating the Master Mold and Angled Microflap Array. The process of fabricating the master mold starts with the formation of a thin epoxy film (SU8, Microchem, thickness ~30 μm) as an adhesive layer on a transparent glass substrate (Micro glass substrate, MATSUNAMI). The thin epoxy film formed with flood UV exposure and PEB prevents a thick SU8 layer from delaminating from the transparent glass substrate during the development process. The transparent substrate reduces undesirable reflected paths of UV light during angled exposure. Further spin-casting leads to a thick PR layer (SU8, Microchem; thickness ~80 μm) on the epoxy layer. Exposure of the thick layer of the negative PR (SU8 2075, Microchem; thickness ~80 μm) twice at different angles of 65° and 72° through one photomask leads to angled walls of 45° and 60°, respectively, by Snell's law from a horizontal plane. See the details in the SI. PEB and development remove the unexposed regions. Rinsing with isopropyl alcohol completes the process for the master mold. The array of angled microflaps is formed by casting and curing of the 10:1 mixture of PDMS base and curing agent (Sylgard 184, Dow Corning) into the master mold. Degassing the mixture, which was poured into the master mold in a vacuum chamber for 30 min, removes air bubbles. Peeling the angled microflap array carefully after it is cured in an oven at 70 °C for 90 min completes the process.

Measuring the Mechanical Characteristics. We measured the mechanical characteristics, i.e., the normal and shear forces, of the angled microflap array when making contact to and retracting from a substrate using the custom-built three-dimensional motorized stage and multiaxis force sensor as described elsewhere.[23] After alignment of an array of the angled microflap array (5 mm × 5 mm) parallel to a substrate using the dual-axis tilting stage, we ran the motorized stage to follow the predetermined paths, e.g., approach normal to the substrate and retract with the desired angles while collecting measurement data and normal and shear forces with a data acquisition board (NI-7330 and NI X-series, NI instrument) with a sampling rate of 100 Hz. The applied preloads, retraction angles, and speed are programmable. The contact areas are also monitored with a stereomicroscope (SZX7, Olympus).

Fabricating the Micrometer-Scale Si Membranes. Dry and wet chemical etching of SOI wafers (Si 7 μm; buried oxide 1 μm) with a mask of PR prepares the micrometer-scale Si membranes for transfer-printing. The process starts with the formation of various shapes in different sizes with a PR (AZ5214; thickness ~1.8 μm), followed by inductively coupled plasma reactive ion etching (Plasma lab 100, Oxford instruments) of the top Si down to the oxide layer. A buffered oxide etching solution (BOE 6:1; J.T. Baker) removes the oxide slightly (width ~1 μm) under the boundary of the top Si after the exposed oxide layer is removed completely for 10 min. The narrow undercut of the oxide layer around the circumference of the Si membranes provides space for liquid PR to fill into. Flood exposure and development of a layer of PR (AZ5214) spun on the sample leaves only the narrow PR (width ~1 μm) under the boundary of the Si membranes. The PR holds the Si membranes temporarily even after the underlying oxide layer is removed in HF (49%, J. T. Baker) for 60–120 min (etch rate ~1.8 μm/min at 25 °C). See more details in the SI.

Transfer-Printing the Micrometer-Scale Si Membranes. Automatic picking up and placing of the membranes is programmed into the custom-built automatic stage equipped with the multiaxis force sensor based on the mechanical characteristics of the angled microflap arrays. The automatic stage approaches, makes contact, and preloads the micrometer-scale Si membrane up to the predefined value (1 N) in the normal direction and then retracts at the angle (retraction angle 60–70°) that provides maximum adhesion for picking up the micrometer-scale Si membrane at a relatively fast speed (retraction speed 200 μm/s). After the original substrate is replaced with the receiver substrate, the automatic stage approaches to make contact until the preload reaches 1 N in the normal direction and retracts at a relatively slow speed (50 μm/s) at the angle (100°) that generates low adhesion to release the micrometer-scale Si membranes on the receiver substrate. The progress of transfer-printing is monitored and recorded with a digital camera mounted in a stereomicroscope.

■ ASSOCIATED CONTENT

Ⓢ Supporting Information

Illustration of the fabrication process, images of angled exposure, image of the custom printing stage, images of the angled microflaps under preload, image of vertically aligned micrometer-scale Si membranes, schematic illustration for the preparation of Si membranes, and a video for automated transfer-printing. This material is available free of charge via the Internet at http://pubs.acs.org.

■ AUTHOR INFORMATION

Corresponding Author

*E-mail: jong@gist.ac.kr.

Author Contributions

The manuscript was written through contributions of all authors. All authors have given approval to the final version of the manuscript.

Notes

The authors declare no competing financial interest.

■ ACKNOWLEDGMENTS

This work was supported by a National Research Foundation of Korea grant funded by the Korean government (Grant 2013007512).

■ REFERENCES

(1) Park, S.-I.; Xiong, Y.; Kim, R.-H.; Elvikis, P.; Meitl, M.; Kim, D.-H.; Wu, J.; Yoon, J.; Yu, C.-J.; Liu, Z.; Huang, Y.; Hwang, K.; Ferreira, P.; Li, X.; Choquette, K.; Rogers, J. A. Printed Assemblies of Inorganic Light-Emitting Diodes for Deformable and Semitransparent Displays. *Science* **2009**, *325*, 977–981.

(2) Kim, H.; Brueckner, E.; Song, J. Unusual Strategies for Using Indium Gallium Nitride Grown on Silicon (111) for Solid-State Lighting. *Proc. Natl. Acad. Sci. U. S. A.* **2011**, *108*, 10072–10077.

(3) Kim, R.-H.; Kim, S.; Song, Y. M.; Jeong, H.; Kim, T.; Lee, J.; Li, X.; Choquette, K. D.; Rogers, J. A. Flexible Vertical Light Emitting Diodes. *Small* **2012**, *8*, 3123–3128.

(4) Lee, J.; Wu, J.; Shi, M.; Yoon, J.; Park, S.-I.; Li, M.; Liu, Z.; Huang, Y.; Rogers, J. A. Stretchable GaAs Photovoltaics with Designs That Enable High Areal Coverage. *Adv. Mater.* **2011**, *23*, 986–991.

(5) Lee, J.; Wu, J.; Ryu, J. H.; Liu, Z.; Meitl, M.; Zhang, Y.-W.; Huang, Y.; Rogers, J. A. Stretchable Semiconductor Technologies with High Areal Coverages and Strain-Limiting Behavior: Demonstration in High-Efficiency Dual-Junction GaInP/GaAs Photovoltaics. *Small* **2012**, *8*, 1851–1856.

(6) Kim, D.-H.; Viventi, J.; Amsden, J. J.; Xiao, J.; Vigeland, L.; Kim, Y.-S.; Blanco, J. A.; Panilaitis, B.; Frechette, E. S.; Contreras, D.; Kaplan, D. L.; Omenetto, F. G.; Huang, Y.; Hwang, K.-C.; Zakin, M. R.; Litt, B.; Rogers, J. A. Dissolvable Films of Silk Fibroin for Ultrathin Conformal Bio-Integrated Electronics. *Nat. Mater.* **2010**, *9*, 511–517.

(7) Kim, D.-H.; Lu, N.; Ghaffari, R.; Rogers, J. A. Inorganic Semiconductor Nanomaterials for Flexible and Stretchable Bio-Integrated Electronics. *NPG Asia Mater.* **2012**, *4*, e15.

(8) Koo, J. H.; Seo, J.; Lee, T. Nanomaterials on Flexible Substrates to Explore Innovative Functions: From Energy Harvesting to Bio-Integrated Electronics. *Thin Solid Films* **2012**, *524*, 1–19.

(9) Wang, C.; Zheng, W.; Yue, Z.; Too, C. O.; Wallace, G. G. Buckled, Stretchable Polypyrrole Electrodes for Battery Applications. *Adv. Mater.* **2011**, *23*, 3580−3584.

(10) Xu, S.; Zhang, Y.; Cho, J.; Lee, J.; Huang, X.; Jia, L.; Fan, J. A.; Su, Y.; Su, J.; Zhang, H.; Cheng, H.; Lu, B.; Yu, C.; Chuang, C.; Kim, T.-I.; Song, T.; Shigeta, K.; Kang, S.; Dagdeviren, C.; Petrov, I.; Braun, P. V.; Huang, Y.; Paik, U.; Rogers, J. A. Stretchable Batteries with Self-Similar Serpentine Interconnects and Integrated Wireless Recharging Systems. *Nat. Commun.* **2013**, *4*, 1543.

(11) Lacour, S. P.; Jones, J.; Wagner, S. Stretchable Interconnects for Elastic Electronic Surfaces. *Proc. IEEE* **2005**, *93*, 1459−1467.

(12) Gonzalez, M.; Axisa, F.; Vanden Bulcke, M.; Brosteaux, D.; Vandevelde, B.; Vanfleteren, J. Design of Metal Interconnects for Stretchable Electronic Circuits. *Microelectron. Reliab.* **2008**, *48*, 825−832.

(13) Choi, K. M.; Rogers, J. A. A Photocurable Poly(dimethylsiloxane) Chemistry Designed for Soft Lithographic Molding and Printing in the Nanometer Regime. *J. Am. Chem. Soc.* **2003**, *125*, 4060−4061.

(14) Kim, T.; Kim, M. J.; Jung, Y. H.; Jang, H.; Dagdeviren, C.; Pao, H. A.; Cho, S. J.; Carlson, A.; Yu, K. J.; Ameen, A.; Chung, H.; Jin, S. H.; Ma, Z.; Rogers, J. A. Thin Film Receiver Materials for Deterministic Assembly by Transfer Printing. *Chem. Mater.* **2014**, *26*, 3502−3507.

(15) Tsao, C.-W.; DeVoe, D. L. Bonding of Thermoplastic Polymer Microfluidics. *Microfluid. Nanofluid.* **2008**, *6*, 1−16.

(16) Li, Y.; Wong, C. P. Recent Advances of Conductive Adhesives as a Lead-Free Alternative in Electronic Packaging: Materials, Processing, Reliability and Applications. *Mater. Sci. Eng., R* **2006**, *51*, 1−35.

(17) Autumn, K.; Sitti, M.; Liang, Y. a; Peattie, A. M.; Hansen, W. R.; Sponberg, S.; Kenny, T. W.; Fearing, R.; Israelachvili, J. N.; Full, R. J. Evidence for van Der Waals Adhesion in Gecko Setae. *Proc. Natl. Acad. Sci. U. S. A.* **2002**, *99*, 12252−12256.

(18) Tian, Y.; Pesika, N.; Zeng, H.; Rosenberg, K.; Zhao, B.; McGuiggan, P.; Autumn, K.; Israelachvili, J. Adhesion and Friction in Gecko Toe Attachment and Detachment. *Proc. Natl. Acad. Sci. U. S. A.* **2006**, *103*, 19320−19325.

(19) Chan, E. P.; Smith, E. J.; Hayward, R. C.; Crosby, A. J. Surface Wrinkles for Smart Adhesion. *Adv. Mater.* **2008**, *20*, 711−716.

(20) Ko, H.; Zhang, Z.; Chueh, Y.-L.; Ho, J. C.; Lee, J.; Fearing, R. S.; Javey, A. Wet and Dry Adhesion Properties of Self-Selective Nanowire Connectors. *Adv. Funct. Mater.* **2009**, *19*, 3098−3102.

(21) Murphy, M. P.; Aksak, B.; Sitti, M. Gecko-Inspired Directional and Controllable Adhesion. *Small* **2009**, *5*, 170−175.

(22) Boesel, L. F.; Greiner, C.; Arzt, E.; del Campo, A. Gecko-Inspired Surfaces: A Path to Strong and Reversible Dry Adhesives. *Adv. Mater.* **2010**, *22*, 2125−2137.

(23) Seo, S.; Lee, J.; Kim, K.-S.; Ko, K. H.; Lee, J. H.; Lee, J. Anisotropic Adhesion of Micropillars with Spatula Pads. *ACS Appl. Mater. Interfaces* **2014**, *6*, 1345−1350.

(24) Kim, S.; Spenko, M. Smooth Vertical Surface Climbing with Directional Adhesion. *IEEE Trans. Rob.* **2008**, *24*, 1−10.

(25) Murphy, M. P.; Kute, C.; Menguc, Y.; Sitti, M. Waalbot II: Adhesion Recovery and Improved Performance of a Climbing Robot Using Fibrillar Adhesives. *Int. J. Rob. Res.* **2010**, *30*, 118−133.

(26) Krahn, J.; Liu, Y.; Sadeghi, A.; Menon, C. A Tailless Timing Belt Climbing Platform Utilizing Dry Adhesives with Mushroom Caps. *Smart Mater. Struct.* **2011**, *20*, 115021.

(27) Gillies, A. G.; Kwak, J.; Fearing, R. S. Controllable Particle Adhesion with a Magnetically Actuated Synthetic Gecko Adhesive. *Adv. Funct. Mater.* **2013**, *23*, 3256−3261.

(28) Lee, J.; Fearing, R. S. Contact Self-Cleaning of Synthetic Gecko Adhesive from Polymer Microfibers. *Langmuir* **2008**, *24*, 10587−10591.

(29) Jeong, H. E.; Lee, J.-K.; Kwak, M. K.; Moon, S. H.; Suh, K. Y. Effect of Leaning Angle of Gecko-Inspired Slanted Polymer Nanohairs on Dry Adhesion. *Appl. Phys. Lett.* **2010**, *96*, 043704.

(30) Lee, J.; Fearing, R. S. Wet Self-Cleaning of Superhydrophobic Microfiber Adhesives Formed from High Density Polyethylene. *Langmuir* **2012**, *28*, 15372−15377.

(31) Dening, K.; Heepe, L.; Afferrante, L.; Carbone, G.; Gorb, S. Adhesion Control by Inflation: Implications from Biology to Artificial Attachment Device. *Appl. Phys. A: Mater. Sci. Process.* **2014**, 567−573.

(32) Yoon, H.; Woo, H.; Choi, M. K.; Suh, K. Y.; Char, K. Face Selection in One-Step Bending of Janus Nanopillars. *Langmuir* **2010**, *26*, 9198−9201.

(33) Yoon, H.; Jeong, H. E.; Kim, T.; Kang, T. J.; Tahk, D.; Char, K.; Suh, K. Y. Adhesion Hysteresis of Janus Nanopillars Fabricated by Nanomolding and Oblique Metal Deposition. *Nano Today* **2009**, *4*, 385−392.

(34) Choi, M. K.; Yoon, H.; Lee, K.; Shin, K. Simple Fabrication of Asymmetric High-Aspect-Ratio Polymer Nanopillars by Reusable AAO Templates. *Langmuir* **2011**, *27*, 2132−2137.

(35) Kim, S.; Wu, J.; Carlson, A.; Jin, S. H.; Kovalsky, A.; Glass, P.; Liu, Z.; Ahmed, N.; Elgan, S. L.; Chen, W.; Ferreira, P. M.; Sitti, M.; Huang, Y.; Rogers, J. A. Microstructured Elastomeric Surfaces with Reversible Adhesion and Examples of Their Use in Deterministic Assembly by Transfer Printing. *Proc. Natl. Acad. Sci. U. S. A.* **2010**, *107*, 17095−17100.

(36) Yang, S. Y.; Carlson, A.; Cheng, H.; Yu, Q.; Ahmed, N.; Wu, J.; Kim, S.; Sitti, M.; Ferreira, P. M.; Huang, Y.; Rogers, J. A. Elastomer Surfaces with Directionally Dependent Adhesion Strength and Their Use in Transfer Printing with Continuous Roll-to-Roll Applications. *Adv. Mater.* **2012**, *24*, 2117−2122.

(37) Mengüç, Y.; Yang, S. Y.; Kim, S.; Rogers, J. A.; Sitti, M. Gecko-Inspired Controllable Adhesive Structures Applied to Micromanipulation. *Adv. Funct. Mater.* **2012**, *22*, 1246−1254.

(38) Sariola, V.; Sitti, M. Mechanically Switchable Elastomeric Microfibrillar Adhesive Surfaces for Transfer Printing. *Adv. Mater. Interfaces* **2014**, *1*, 1300159.

(39) Bartlett, M. D.; Crosby, A. J. Material Transfer Controlled by Elastomeric Layer Thickness. *Mater. Horiz.* **2014**, *1*, 507−512.

(40) Jeong, J.; Kim, J.; Song, K.; Autumn, K.; Lee, J. Geckoprinting: Assembly of Microelectronic Devices on Unconventional Surfaces by Transfer Printing with Isolated Gecko Setal Arrays. *J. R. Soc. Interface* **2014**, *11*, 20140627.

(41) Rosqvist, T.; Johansson, S. Soft Micromolding and Lamination of Piezoceramic Thick Films. *Sens. Actuators, A* **2002**, *98*, 512−519.

(42) Wolf, K. B.; Krotzsch, G. Geometry and Dynamics in Refracting Systems. *Eur. J. Phys.* **1995**, *16*, 14−20.

(43) del Campo, A.; Greiner, C. SU-8: A Photoresist for High-Aspect-Ratio and 3D Submicron Lithography. *J. Micromech. Microeng.* **2007**, *17*, R81−R95.

(44) Birch, K.; Downs, M. An Updated Edlén Equation for the Refractive Index of Air. *Metrologia* **1993**, *30*, 155−162.